

Dielectric susceptibility of quantum Ising model: Simulated monoclinic A_2BX_4 -type ferroelectrics

Hiroyuki Mashiyama^{1*}, Hirotake Shigematsu², and Takanao Asahi³

¹*Yamaguchi University, Yamaguchi 753-8511, Japan*

²*Faculty of Education, Yamaguchi University, Yamaguchi 753-8513, Japan*

³*Graduate School of Sciences and Technology for Innovation, Yamaguchi University, Yamaguchi 753-8512, Japan*

*E-mail: mashi@yamaguchi-u.ac.jp

To explain the anomalous increase in the permittivity of monoclinic Rb_2ZnI_4 at low temperatures, the dielectric susceptibilities of modulated structures are calculated. A quantum Ising model is reduced from a lattice Hamiltonian by the mean field approximation and two-quantum-level approximation. The susceptibilities of modulated phases remain to be finite values at zero temperature as in the uniform ferroelectric phase, if the quantum effect works. Furthermore, the susceptibilities of the incommensurate and high-order commensurate phases increase at low temperatures. Since the ferroelectric phase can be realized with accompanying strong discontinuity, such an increase is different from the phenomenon during the lock-in transition. The phase diagram and the temperature dependence of susceptibility are calculated. With the selection of a proper set of parameters, the theoretical results agree qualitatively with experimental reports of $(Rb_{1-x}K_x)_2ZnI_4$.

1. Introduction

A high dielectric permittivity is one of the useful properties of ferroelectric materials in applications.¹⁾ The temperature dependence of dielectric susceptibility can be described by the Curie-Weiss law in proper ferroelectrics, which predicts that the permittivity diverges in second-order transitions.^{2,3)} The presence of ferroelectric domains additionally contribute to the permittivity in ferroelectric phases.⁴⁾

On the other hand, the permittivity shows slight changes during the phase transition of improper ferroelectrics, in which the order parameter of the phase transition is not a dielectric moment but another quantity coupled with the dielectric moment.⁵⁾ In the case of incommensurate crystals, the permittivity increases considerably during the lock-in transition between incommensurate and commensurate (ferroelectric) phases, even though the commensurate phase is an improper ferroelectric state.⁶⁻¹⁰⁾ Such a case is observed in K_2SeO_4 ,^{11,12)} Rb_2ZnCl_4 ,¹³⁾ and isomorphous A_2BX_4 crystals with the similar orthorhombic structure.¹⁴⁾ The abnormal increase in the permittivity can be attributed to movable discommensurations in the incommensurate phase and the residual domain walls in the commensurate phase.^{15,16)}

Although the chemical formula is the same as that of A_2BX_4 , K_2ZnI_4 has a different monoclinic morphology and undergoes the proper ferroelectric transition at 270 K accompanying the Curie-Weiss behavior of the permittivity.¹⁷⁾ The isomorphous Rb_2ZnI_4 was investigated previously; the temperature dependence of the permittivity somehow resembles that in K_2SeO_4 , but no ferroelectricity was detected below the reported second transition at 7.5 K.¹⁸⁾ The crystal is paraelectric in the entire temperature range. The cusplike anomaly at 62.4 K was later found to be the incommensurate transition.^{19,20)} The modulation wave number is about 0.3 referring to the pseudo-orthorhombic cell.²¹⁾ No lock-in transition is observed at low temperatures.

Rb_2ZnI_4 was reinvestigated later.²⁰⁾ Its permittivity showed a peak at approximately 4 K, if the applied electric field was in the radio frequency range. However, the permittivity saturated gradually toward 0 K, if static measurement was performed. Down to 1.4 K, no ferroelectricity nor pyroelectricity was detected,²⁰⁾ and the behavior resembles the quantum paraelectricity of SrTiO_3 .^{22,23)}

To elucidate the low-temperature state of Rb_2ZnI_4 , a mixed crystal system of $(\text{Rb}_1-$

$x\text{K}_x)_2\text{ZnI}_4$ has been investigated recently.^{20,24,25)} With the increasing substitution ratio x , the incommensurate transition temperature from the disordered phase (the paraelectric room-temperature phase) increases gradually. The ferroelectric phase appears at low temperatures, if $x \geq 0.14$. With the further increase in x , the transition temperature to the ferroelectric phase increases, and finally the paraelectric-ferroelectric transition takes place directly for $x > 0.4$ as in pure K_2ZnI_4 .

It is plausible that Rb_2ZnI_4 shows an increased permittivity with the approaching commensurate phase of $q = 0$ (the proper ferroelectric state) at low temperatures, similarly to the lock-in transitions of K_2SeO_4 or Rb_2ZnCl_4 .¹²⁻¹⁵⁾ However, this will not be the case, because the transition from the incommensurate phase with $q \sim 0.3$ to the commensurate phase with $q=0$ is strongly first-order. Therefore, Takashige *et al.* suggested that the phenomenon was similar to quantum paraelectricity.²⁰⁾

To explain the dielectric susceptibility of an incommensurate phase, thermodynamic functions (phenomenological free energy) with the additional Lifshitz invariant were investigated previously.⁶⁻¹⁰⁾ Such phenomenological explanations were based on classical thermodynamics. The quantum effect can be considered in the paraelectric phase using microscopic or semimicroscopic consideration.^{23,26)} In the proper ferroelectric phase, a quasi-harmonic approximation^{27,28)} or a two-level approximation²⁹⁻³²⁾ was useful in theoretical analysis. Quantum paraelectricity is usually described by the Barrett's equation of dielectric susceptibility; the equation was derived theoretically for paraelectric-ferroelectric (proper) transitions previously.

In Rb_2ZnI_4 , not the disordered phase, but the incommensurate phase, displays the increased permittivity at low temperature.²⁰⁾ To examine the modulated phases, we have to consider models of incommensurate structures. A typical one is the Ising model with competing interactions.³³⁾ The model was investigated extensively and named axial next-nearest neighbor Ising model (ANNNI), which contained first- and second-nearest-neighbor interactions.³⁴⁾ The revised one was extended to third-nearest-neighbor interactions.³⁵⁻³⁷⁾ If such ANNNI models were analyzed using classical thermodynamics, then the modulated structures at zero temperature were commensurate phases, and the incommensurate phase was stable only at a finite temperature.³⁴⁻³⁷⁾

Previously, we analyzed the ANNNI model using quantum thermodynamics. We found

that the incommensurate phases may extend down to zero temperature.²¹⁾ Therefore, the quantum ANNNI model can describe the phase diagram of the mixed system of $(\text{Rb}_{1-x}\text{K}_x)_2\text{ZnI}_4$. However, the dielectric susceptibility of modulated structures in the quantum ANNNI model has not been calculated so far. Within the theoretical framework, the dielectric susceptibility was calculated only for the paraelectric-ferroelectric ($q = 0$) transition.³²⁾ Whether the peculiar permittivity of Rb_2ZnI_4 can be explained theoretically or not requires further analysis.

Here, we would like to note that quantum effects on ferroelectrics have also been the focus of much interest recently for developing novel ferroelectric materials.^{38,39)} Therefore, the analysis of quantum effects would provide useful insights into ferroelectricity in both fundamentals and applications.

This paper is devoted to the calculation of dielectric susceptibility in modulated phases. Firstly, a lattice Hamiltonian including an unharmonic self-potential is presented after the model of previous works.^{3,21,32,40)} A quantum two-level approximation and the mean field approximation reduce the Hamiltonian to the quantum ANNNI model. Although the free energy of the quantum ANNNI model was presented previously, we briefly summarize the formulation in the next section. The permittivity is then derived within linear responses against the applied external field.

By choosing the appropriate set of effective interaction parameters, the phase diagram and the temperature dependence of dielectric susceptibility are obtained by numerical computations in Sect. 3. To explain the mixed system of $(\text{Rb}_{1-x}\text{K}_x)_2\text{ZnI}_4$ successfully, an ambitious assumption of parameters will be introduced. In Sect. 4, we present some conclusions.

2. Model and formulation

The Hamiltonian of lattice vibrations is written as

$$H = \frac{1}{2} \sum_{q,s} \left(\dot{Q}_q^{(s)} \dot{Q}_{-q}^{(s)} + \omega(q;s)^2 Q_q^{(s)} Q_{-q}^{(s)} \right) , \quad (1)$$

where $Q_q^{(s)}$ is a normal coordinate of the wave number q and the mode is classified by s .^{3,21)} In the following, we consider only one mode relevant to the ferroelectric transition and omit the superscript s hereafter. The Hamiltonian Eq. (1) for the mode can be rewritten as

$$H = \frac{1}{2} \sum_n (\dot{x}_n^2 - \sum_l J_l x_n x_{n+l}) . \quad (2)$$

Here, a local coordinate is given by

$$x_n = \frac{1}{\sqrt{N}} \sum_q Q_q e^{2\pi i q R_n} , \quad (3)$$

which represents the phonon wave pattern on the n -th unit cell. We are concerned with the one-dimensional transverse mode explicitly. The interlayer interaction J_l is a Fourier transform of the phonon energy Eq. (1).

$$J_l = -\frac{1}{2} \sum_q \omega(q)^2 e^{2\pi i q (R_{n+l} - R_n)} \quad (4)$$

To permit a phase transition in the system, let us introduce a self-potential $V(x)$ into Eq. (2):^{3,21,32,40}

$$H = \sum_n \left(\frac{1}{2} \dot{x}_n^2 + V(x_n) - x_n h \right) - \frac{1}{2} \sum_{n,l} J_l x_n x_{n+l} , \quad (5)$$

where h is an external field conjugate to x_n . We assume that the self-potential is unharmonic but is symmetric: $V(-x) = V(x)$, so that the expectation value $\langle x_n \rangle = 0$ at a high temperature.

We adopt two approximations similar to the case of nearest-neighbor interactions:³² (i) the mean field approximation

$$J_l x_n x_{n+l} \longrightarrow J_l x_n \langle x_{n+l} \rangle , \quad (6)$$

and (ii) two-quantum-level approximation. Without h and J_l , the single-particle Hamiltonian Eq. (5) can be solved in principle, and energy levels higher than 2 (ϵ_m ; $m \geq 2$) are neglected at low temperatures. Then, we can derive analytical expressions for the free energy and other thermodynamic quantities, which contain the quantum parameter $T_1 \equiv (\epsilon_1 - \epsilon_0)/k_B$, a representative of the energy gap of the single-particle Hamiltonian.^{21,32} The Boltzmann constant k_B is set to 1, hereafter.

We write the free energy on the basis of our previous paper as²¹)

$$F = \frac{1}{2} \sum_{n,l} J_l \xi_n \xi_{n+l} - T \sum_n \ln \left(2 \cosh \frac{\Lambda_n}{T} \right) . \quad (7)$$

Here, $\xi_n \equiv \langle x_n \rangle / \|x\|$ is the order parameter normalized by the quantum expectation value, which is set to 1 in length unit, hereafter.²¹) The mean field is given by

$$\Lambda_n = \sqrt{(T_1/2)^2 + (h + h_n)^2} , \quad (8)$$

with

$$h_n = \sum_l J_l \xi_{n+l} . \quad (9)$$

The obtained relations are equivalent to those of the Ising model with a transverse field,^{29,30} but the interactions extend further than those in second-nearest neighbors. Therefore, the system is called the quantum ANNNI model in this paper.

The Fourier component of the interactions in Eq. (4) can be written as

$$J(q) = \sum_l J_l e^{2\pi i q l} = J_0 + 2(J_1 \cos 2\pi q + J_2 \cos 4\pi q + J_3 \cos 6\pi q + \dots). \quad (10)$$

We truncate up to J_3 , because many incommensurate ferroelectrics can be described by this restriction qualitatively.^{21,34,36} An ordered structure with the wave number q is represented by Fourier components as

$$\xi_n = \sum_k \xi_k e^{2\pi i k q n} = A_1 \cos 2\pi q(n + \nu) + A_3 \cos 6\pi q(n + \nu) + \dots \quad (11)$$

The phase shift ν is $1/2$ for $q = 1/2, 1/4, 1/8$, etc., and 0 in other cases. The free energy is also written as $\{A_k\}$ and is minimized analytically or numerically to fix the amplitudes $\{A_k\}$ for the given wave number q . The primary amplitude $A_1(q)$ appears spontaneously below the transition temperature $T_c(q)$. For the given parameters J_l and T_1 , the structure with the minimum free energy is stable among modulated structures.²¹⁾

If the external field h is switched on, additional even terms should be added to Eq. (11),

$$\delta \xi_n = \delta A_0 + \delta A_2 \cos 4\pi q(n + \nu) + \delta A_4 \cos 8\pi q(n + \nu) + \dots \quad (12)$$

We consider a linear response to h , then the induced δA_k 's obey the following relations:

$$\sum_{k=0,2,\dots} [\Lambda_n - \Xi_n J(kq)] \cos 2\pi k q(n + \nu) \delta A_k = \Xi_n h, \quad (13)$$

where

$$\Xi_n = -\frac{h_n \xi_n}{\Lambda_n} + \tanh \frac{\Lambda_n}{T} + \frac{h_n^2}{T \Lambda_n} \operatorname{sech}^2 \frac{\Lambda_n}{T}, \quad (14)$$

and the coefficients Λ_n and Ξ_n are given by A_k 's under zero field. Since n may be 1 to N (the commensurate cell period), Eq. (13) shows linear equations for δA_k 's. If q is incommensurate, the number of Fourier amplitudes is infinity in principle. We truncate them at 5 or 10 orders and replace discrete summations by integrations.²¹⁾ Thus, it is solved algebraically, once the zero-field order parameters ξ_n 's are fixed. The susceptibility for the uniform external field is obtained as

$$\chi = \delta A_0 / h. \quad (15)$$

In the disordered (paraelectric) phase, the susceptibility is identical to Barrett's equation:^{23,26)}

$$\chi = \left[\frac{T_1}{2} \coth \frac{T_1}{2T} - J(0) \right]^{-1}. \quad (16)$$

Generally, the calculations to minimize free energy and obtain Fourier components and susceptibility are performed numerically.

3. Results and discussion

If we apply the formulations to incommensurate phases of thiourea ($J_1 > 0$, $J_2 < 0$) and orthorhombic A_2BX_4 systems ($J_1 < 0$, $J_2 < 0$), then the increase in permittivity accompanying lock-in transitions can be simulated successfully. However, in the following, we apply another case to clarify the quantum effect on modulated crystals.

3.1 Phase diagram

In our previous paper,²¹⁾ we considered the quantum effect on the phase diagram for the interaction parameters $J_1 = 1$, $J_2 < 0$, and $J_3 > 0$ in the discussion of the phase transition of monoclinic A_2BX_4 .²⁰⁾ We demonstrated successfully that the incommensurate phase with the wave number ca. 0.3 extends down to zero temperature and the regions of commensurate phases shrink owing to the quantum effect. However, the parameter J_0 was ignored in that paper.

Here, we take J_0 into account and reconstruct the phase diagram. The magnitude of the nearest-neighbor interaction J_1 is set to 1 for the scale of energy/temperature. The other parameters are $J_0 = 2$, $J_3 = 1.5$, and $-3 < J_2 < -0.5$ in the phase diagram of Fig. 1. At high temperatures, the system is disordered, as denoted by ‘PARA’. At low temperatures, ordered states with incommensurate or commensurate wave numbers are stabilized. The period of the commensurate states is limited to 10 unit cells for simplicity, and the longer-period structures are regarded as the incommensurate state denoted by ‘INCOM’. If the system is classical, i.e., the quantum parameter $T_1 = 0$, then the zero temperature states are commensurate phases $q = 0$, $1/3$, $2/7$, and $1/4$; no incommensurate state, as well as $q = 3/10$ commensurate state, survives at zero temperature. The classical phase boundaries are indicated by broken lines in Fig. 1.

When the quantum parameter is switched on, the phase boundaries shift to lower temperatures as shown by solid lines in Fig. 1 for $T_1 = 5$. Note that the regions of $q = 1/3$, $2/7$, and $1/4$ are narrow, and the regions of the incommensurate state and commensurate $q = 3/10$ state enlarge and reach the axis of zero temperature.

3.2 Dielectric susceptibilities

The susceptibility χ defined by Eq. (15) represents the dielectric susceptibility if the local coordinate x_n belongs to the polar symmetry and the external field is an electric one. Therefore, χ will demonstrate the permittivity of a nominally single crystal. The calculated susceptibility χ is plotted in Fig. 2 as a function of temperature T , where T_1 , J_0 , J_1 , and J_3 are

5, 2, 1, and 1.5, respectively. The value of the parameter J_2 is shown in the figure. The cusps at approximately $T = 6$ indicate PARA-INCOM transitions. The INCOM phase discontinuously transforms to $q = 1/3$ ($J_2 = -1.1$), $3/10$ ($J_2 = -1.6$), or $2/7$ followed by $1/4$ ($J_2 = -2.4$). If the system is classical ($T_1 = 0$), χ decreases monotonically to zero as temperature decreases. However, quantum fluctuations increase the susceptibility even at low temperatures, so that χ remains at a finite value even at $T = 0$ in both incommensurate and commensurate states. A marked increase in χ is recognized at approximately $T = 3$ in the commensurate phase of $q = 3/10$ for $J_2 = -1.6$. The system remains INCOM, but χ is maximum at $T = 0$ if the INCOM phase reaches $T = 0$, as shown in the case of $J_2 = -2$. The marked increase in incommensurate χ is also recognized for $J_2 = -1.1$ at low temperatures before the transition to the $q = 1/3$ state.

3.3 Simulation of $(\text{Rb}_{1-x}\text{K}_x)_2\text{ZnI}_4$ system

The ferroelectric crystal of K_2ZnI_4 shows a typical paraelectric-ferroelectric transition at T_c , which may correspond to $-0.9 < J_2$ in Fig. 1. On the other hand, Rb_2ZnI_4 undergoes the paraelectric-incommensurate transition at a temperature lower than that in the ferroelectric transition of K_2ZnI_4 . To simulate the mixed crystal system of $(\text{Rb}_{1-x}\text{K}_x)_2\text{ZnI}_4$, let us introduce a simple but arbitrary assumption for the parameter,

$$J_0 = 4.5 + 4J_2 \quad . \quad (17)$$

Other parameters are set at $T_1 = 2$, $J_1 = 1$, $J_3 = 0.9$, $-1.1 < J_2 < -0.7$. Then the phase diagram is modified as shown in Fig. 3. No commensurate phase except for the ferroelectric phase ($q = 0$) appears. This phase diagram is similar in phase boundaries to $(\text{Rb}_{1-x}\text{K}_x)_2\text{ZnI}_4$ with $x < 0.5$. The incommensurate wave number for $J_2 = -1$ is $q = 0.29$, which fairly agrees with the reported value of 0.3 for Rb_2ZnI_4 . The transition between the incommensurate phase and the commensurate ($q = 0$) phase is a first-order one.

The temperature dependence of the susceptibility is shown in Fig. 4 for three selected J_2 's. For $J_2 = -0.75$, the paraelectric-ferroelectric transition occurs at $T_c = 3.71$, where χ diverges to infinity. With decreasing temperature below T_c , χ decreases monotonically; however, it shows an expanded curvature at around $T \sim 2$. Since the calculation assumes a single domain in the ferroelectric phase, this behavior is caused not by domains but by quantum fluctuations.

For $J_2 = -0.85$, the paraelectric phase transforms to the incommensurate phase with an accompanying cusp anomaly at $T_c = 3.23$, which is followed by the ferroelectric phase below

$T = 2.50$. At $T = 0$, χ of the ferroelectric phase remains finite as mentioned above.

For $J_2 = -0.95$, the paraelectric phase transforms to the incommensurate phase at $T_c = 2.99$, below which the incommensurate phase is stable down to zero temperature. The susceptibility χ takes a minimum value at around $T = 1.15$, and it grows slightly in the low-temperature range. The value saturates at 140% of the local minimum. Such an increase in χ qualitatively resembles the temperature dependence of the permittivity of Rb_2ZnI_4 (Fig. 1 in Ref. 20 and Figs. 2 and 3 in Ref. 24).

4. Conclusions

In SrTiO_3 and related perovskite crystals, quantum fluctuations suppress ferroelectricity and the crystals remain in the paraelectric state accompanied by markedly increased permittivity at low temperatures.^{22,23,26} Quantum paraelectricity has been the focus of much interest recently in the field of novel organic ferroelectrics.^{38,39} The similar phase diagram and the increased permittivity in the mixed crystal system $(\text{Rb}_{1-x}\text{K}_x)_2\text{ZnI}_4$ have been reported.^{17,20,24,25} The typical quantum paraelectricity is recognized at the ferroelectric phase transition from the paraelectric phase. However, in the case of $(\text{Rb}_{1-x}\text{K}_x)_2\text{ZnI}_4$, the increased permittivity is observed in the ordered incommensurate phase. To explain the quantum effect on the incommensurate phase, we have analyzed the quantum ANNNI model and calculated the dielectric susceptibility.

The conclusions are summarized as follows: (i) We can reconstruct the phase diagram qualitatively, and the incommensurate state is stable down to zero temperature for some parameter regions. (ii) The incommensurate-ferroelectric transition is a strong first-order transition, so that the susceptibility only changes discontinuously, which is different from the case of the lock-in transitions. (iii) Not only in the incommensurate phase but also in the high-order commensurate phase as $q = 3/10$, the susceptibility tends to increase and saturates at zero temperature. (iv) Because of the quantum effect, the order parameter cannot increase to the classical value, and the parameter can change its magnitude in response to the external field. Such a phenomenon may be called quantum incommensurability as an analogy of quantum paraelectricity.

Finally, let us comment on the chosen parameters. The parameters $\{J_n\}$ do not indicate the bare atomic interactions between neighbors, but only represent the soft mode dispersion [see

Eq. (4)]. Therefore, such a range of $J_3 > J_1 \sim -J_2$ is not peculiar at all. As discussed in our previous paper,²¹⁾ the parameters are set to reproduce the phase diagram where the $q \sim 0.3$ incommensurate phase lies beside the $q = 0$ commensurate phase; that is, the phonon dispersion $\omega(q)$ has two minima at around $q = 0$ and $q \sim 0.3$. Further experimental investigations, especially diffraction studies of Rb_2ZnI_4 and the isomorphous crystals at low temperatures are desirable. In addition, dynamical susceptibility shall be calculated within the mean field approximation, if time-dependent external force and responses are considered.^{3,40,41)}

Acknowledgments

This work was partially supported by a research grant category A1-2(2017) from the Yamaguchi University Foundation. The authors are grateful to Professors M. Takashige and T. Yamaguchi of Meisei University for many helpful discussions.

References

- 1) H. Taniguchi, K. Ando, and I. Terasaki, *Jpn. J. Appl. Phys.* **56**, 10PC02 (2017).
- 2) T. Mitsui, I. Tatsuzaki, and E. Nakamura, *An Introduction to the Physics of Ferroelectric* (Gordon and Breach, New York, 1976) Chap. 2.
- 3) M. E. Lines and A. M. Glass, *Principles and Applications of Ferroelectrics and Related Materials* (Oxford University Press, Oxford, UK, 1977) Chaps. 2 and 3.
- 4) B. A. Strukov and A. P. Levanyuk, *Ferroelectric Phenomena in Crystals: Physical Foundations* (Springer, Berlin, 1998) Chap. 10.
- 5) A. P. Levanyuk and D. G. Sannikov, *Sov. Phys. Usp.* **17**, 199 (1974).
- 6) A. P. Levanyuk and D. G. Sannikov, *Sov. Phys. Solid State* **18**, 1122 (1976).
- 7) W. L. McMillan, *Phys. Rev. B* **14**, 1496 (1976).
- 8) Y. Ishibashi and V. Dvorak, *J. Phys. Soc. Jpn.* **44**, 32 (1978).
- 9) H. Shiba and Y. Ishibashi, *J. Phys. Soc. Jpn.* **44**, 1592 (1978).
- 10) Y. Ishibashi and H. Shiba, *J. Phys. Soc. Jpn.* **45**, 409 (1978).
- 11) K. Aiki, K. Hukuda, H. Koga, and T. Kobayashi, *J. Phys. Soc. Jpn.* **28**, 389 (1970).
- 12) M. Iizumi, J. D. Axe, G. Shirane, and K. Shimaoka, *Phys. Rev.* **15**, 4392 (1977).
- 13) K. Hamano, Y. Ikeda, T. Fujimoto, K. Ema, and S. Hirotsu, *J. Phys. Soc. Jpn.* **49**, 2278 (1980).
- 14) J. D. Axe, M. Iizumi, and G. Shirane, in *Incommensurate Phases in Dielectrics*, ed. R. Blinc and A. P. Levanyuk (North-Holland, Amsterdam, 1986) Vol. 2, Chap. 10.
- 15) A. Levstik, P. Prelovsek, C. Filipic, and B. Zeks, *Phys. Rev. B* **25**, 3416 (1982).
- 16) H. Mashiyama and H.-G. Unruh, *J. Phys. C* **16**, 5009 (1983)
- 17) F. Shimizu, T. Anzai, H. Sekiguchi, M. Takashige, and S. Sawada, *J. Phys. Soc. Jpn.* **63**, 437 (1994).
- 18) K. Geshi, *J. Phys. Soc. Jpn.* **53**, 3850 (1984).
- 19) J. Puragahn, Ph.D. Thesis, Karlsruhe University (1998).
- 20) M. Takashige, T. Yamaguchi, and F. Shimizu, *J. Phys. Soc. Jpn.* **81**, 045001 (2012).
- 21) H. Mashiyama, *J. Phys. Soc. Jpn.* **84**, 104712 (2015).
- 22) E. Sawaguchi, A. Kikuchi, and Y. Kodera, *J. Phys. Soc. Jpn.* **17**, 1666 (1962).
- 23) K. A. Muller and H. Burkard, *Phys. Rev. B* **19**, 3593 (1979).
- 24) T. Yamaguchi, F. Shimizu, and M. Takashige, *Ferroelectrics* **462**, 104 (2014).

- 25) R. Shibata, R. Muraki, T. Yamaguchi, and M. Takashige, *J. Korean Phys. Soc.* **66**, 1367 (2015)
- 26) J. H. Barrett, *Phys. Rev.* **86**, 118 (1952).
- 27) E. K. H. Salje, B. Wruck, and H. Thomas, *Z. Phys. B: Condens. Matter* **82**, 399 (1991).
- 28) S. E. Mkam Tchouobiap and H. Mashiyama, *Phys. Rev. B* **75**, 014101 (2007).
- 29) P. G. de Gennes, *Solid State Commun.* **1**, 132 (1963).
- 30) M. Tokunaga and T. Matsubara, *Prog. Theor. Phys.* **35**, 581 (1966).
- 31) R. Blinc and B. Zeks, *Soft Modes in Ferroelectrics and Antiferroelectrics* (North-Holland, Amsterdam, 1974) Chap. 5.
- 32) H. Mashiyama, S. E. Mkam Tchouobiap, and M. Ashida, *J. Phys. Soc. Jpn.* **77**, 084709 (2008).
- 33) R. J. Elliott, *Phys. Rev.* **124**, 346 (1961).
- 34) P. Bak and J. von Boehm, *Phys. Rev. B* **21**, 5297 (1980).
- 35) S. Katsura and A. Narita, *Prog. Theor. Phys.* **50**, 1750 (1973).
- 36) Y. Yamada and N. Hamaya, *J. Phys. Soc. Jpn.* **52**, 3466 (1983).
- 37) W. Selke, M. Barreto, and J. Yeomans, *J. Phys. C* **18**, L393 (1985).
- 38) S. Horiuchi, K. Kobayashi, R. Kumai, N. Minami, F. Kagawa, and Y. Tokura, *Nat. Commun.* **6**, 7469 (2015).
- 39) F. Kagawa, N. Minami, S. Horiuchi, and Y. Tokura, *Nat. Commun.* **7**, 10675 (2016).
- 40) T. Onodera, *Prog. Theor. Phys.* **44**, 1477 (1970).
- 41) H. Mashiyama, *J. Phys. Soc. Jpn.* **73**, 3466 (2004).

Figure Captions

Fig. 1. (Color online) Calculated phase diagrams for a classical case (broken lines) and a quantum case of $T_1 = 5$ (solid lines). Modulated commensurate phases and uniform phase are shown by $q = 1/4, 2/7, 3/10, 1/3$, and 0. The incommensurately modulated phases denoted by INCOM extend down to zero temperature for the quantum case.

Fig. 2. (Color online) Calculated susceptibility for the quantum case of $T_1 = 5$. The parameters are $J_0 = 2$, $J_1 = 1$, and $J_3 = 1.5$; $J_2 = -1.1, -1.6, -2.0$, and -2.4 are shown in the figure.

Fig. 3. (Color online) Calculated phase diagram with the assumption of $J_0 = 4.5 + 4J_2$. Other parameters are $T_1 = 2$, $J_1 = 1$, and $J_3 = 0.9$.

Fig. 4. (Color online) Temperature T dependence of calculated susceptibility χ with the parameters of $T_1 = 2$, $J_1 = 1$, $J_3 = 0.9$, and $J_0 = 4.5 + 4J_2$. Three cases of J_2 are plotted.

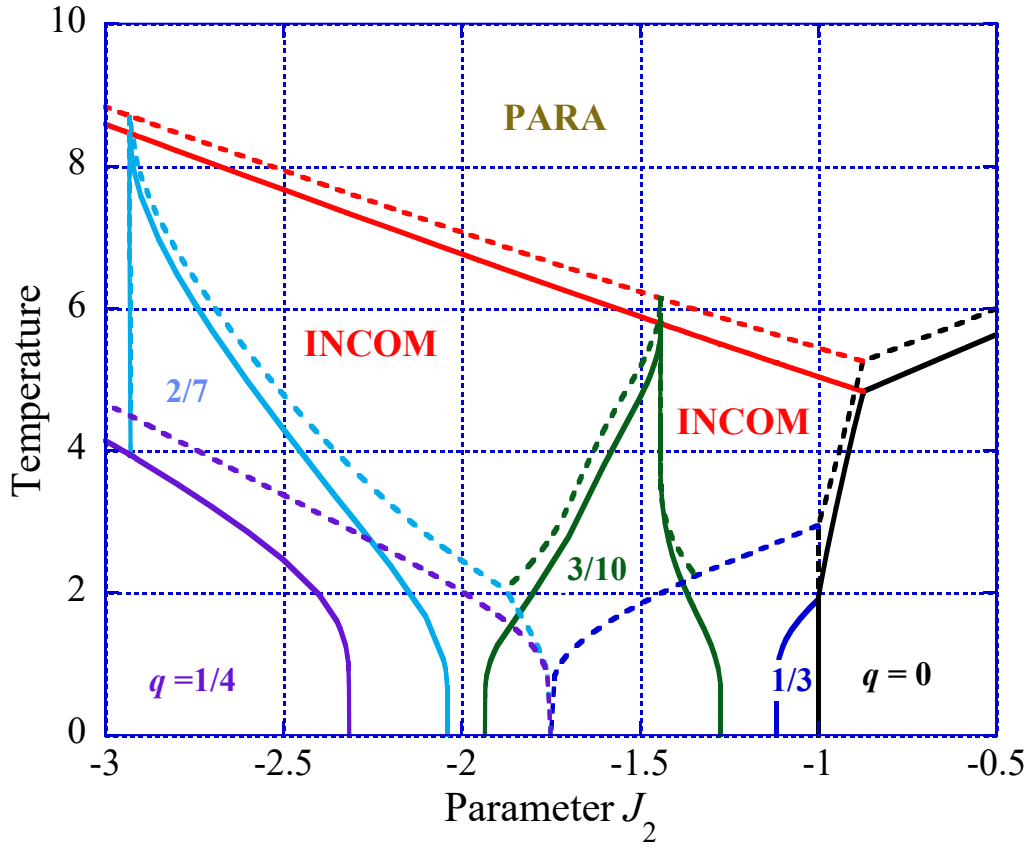


Fig. 1. (Color Online)

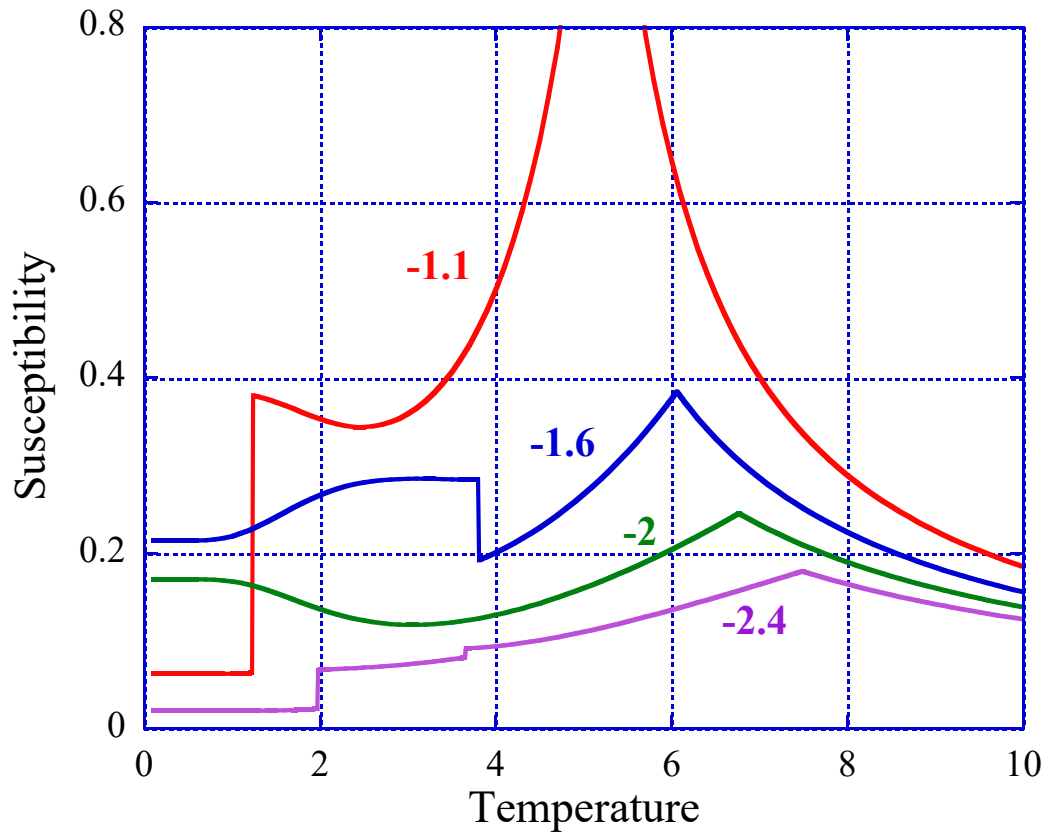


Fig. 2. (Color online)

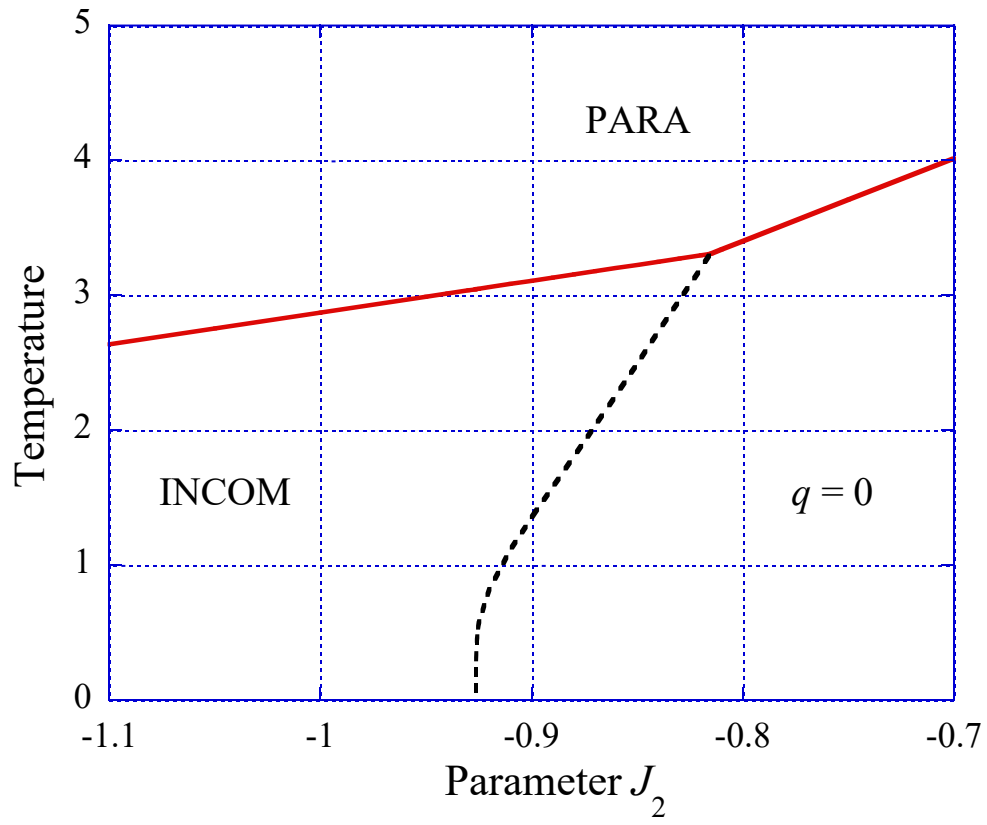


Fig. 3. (Color online)

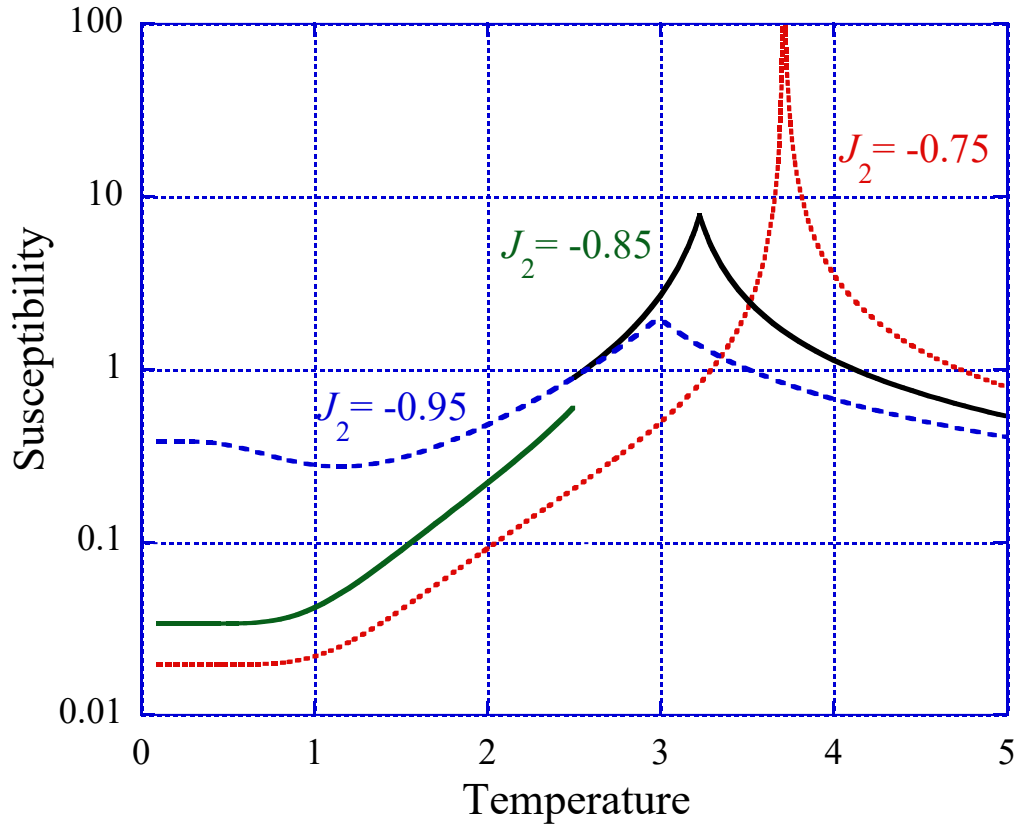


Fig. 4. (Color online)